Gas-Phase Structures, Rotational Barriers, and Conformational Properties of Hydroxyl and Mercapto Derivatives of Cyclohexa-2,5-dienone and Cyclohexa-2,5-dienthione

Miquel Torrent-Sucarrat* and Miquel Solà

Institut de Química Computacional and Departament de Química, Universitat de Girona, E-17071 Girona, Catalonia, Spain

Alejandro Toro-Labbé

Laboratorio de Química Teórica Computacional (QTC), Facultad de Química, Pontificia Universidad Católica de Chile, Casilla 306, Correo 22, Santiago, Chile

Received: January 31, 2006; In Final Form: May 12, 2006

The rotational barriers and conformational properties of the hydroxyl and mercapto groups attached to the α and β positions of cyclohexa-2,5-dione and cyclohexa-2,5-dienthione have been studied at the B3LYP/6-311++G(d,p) level of theory. The results show that the conformational preferences of these studied systems are the result of a subtle interplay between different competing effects (conjugation, hyperconjugation, and steric repulsions). The applicability of the density functional theory reactivity indices and the maximum hardness principle for the present systems has been analyzed.

Introduction

Conjugated polyenes, with alternating double and single bonds, are more stable than their unconjugated counterparts. The extra stabilization of conjugated isomers is a quantum mechanical interaction named conjugation that can be rationalized in valence bond (VB) language using resonant structures and in molecular orbital (MO) theory in terms of $\pi-\pi^*$ interactions. The hyperconjugation[1] is another quantum effect defined as the stabilizing interaction arising from the overlap of an occupied orbital (σ or a lone pair orbital, n) with an empty or partially filled orbital to result in an extended molecular orbital that enhances the stability of the system.[2] Conjugation and hyperconjugation play a fundamental role in the structure and stability of molecules.[3−12] The remarkably short C−C single bond distance in 1,3-butadiene is a structural sign of conjugation, while the increase in the stability of carbocations or radicals with the number of alkyl substituents[13,14] or the preference of 1,2-disubstituted ethanes for the gauche rather than the less steric trans conformation are manifestations of hyperconjugation.[15,16] Further physical evidences of conjugation and hyperconjugation can be obtained from the significant changes of the conformational (distances and angles), spectroscopic (NMR chemical shifts and IR stretching frequencies), and energetic (rotational barriers) properties of molecules, which can be observed and measured with experimental techniques. Finally, the anomeric effect (also known as negative hyperconjugation),[17] which plays an important role in the conformational preferences of a large amount of biochemical systems, has been explained by taking into account $n_\sigma \rightarrow \sigma^*$ and $\sigma \rightarrow \sigma^*$ interactions.[18−21]

A molecular conformation is determined by the interplay between attractive and repulsive interactions that occur in molecules. Among the stabilizing forces, conjugation and hyperconjugation play key roles in the determination of the most favorable conformation. Indeed, hyperconjugation was considered to be the driving force for the staggered equilibrium conformation of ethane,[8] although more recently, other authors have pointed out steric hindrance between vicinal C−H bonds as the dominant factor.[22,23] The conformational preferences (syn or anti forms) of esters, conjugated alcohols, and ethers, which have been the subject of a great deal of experimental and theoretical research,[24−32] are also the result of competing repulsive steric and attractive hyperconjugation interactions. If the steric interaction is the predominant factor, then the most stable structure will be the anti form. On the contrary, the syn form may be the lowest energy conformer if hyperconjugation effects are more important than steric interactions. Finally, it is worth noting that according to Leibold and Oberhammer,[25] the stability of the syn form in vinyl alcohols is mainly due to the conjugation between the oxygen lone pair and its adjacent π double bond ($n_\pi(O) \rightarrow \pi^*(C{=}C)$) and the anomeric effect between $n_\sigma(O)$ and $\sigma^*(C{=}C)$.

The aim of this work is to analyze the energetic barrier and the conjugation and hyperconjugation effects in the internal rotation of the hydroxyl and mercapto groups attached to C2 or C3 of cyclohexa-2,5-dienone and cyclohexa-2,5-dienthione (see Figure 1). Despite their tendency toward rearomatization,[33,34] the cyclohexadienones have been used in a variety of 1,2-additions,[35,36] 1,4-additions,[37,38] rearrangements,[39,40] and cycloaddition reactions.[41,42] Specifically, considerable attention has been given to cyclohexa-2,5-dienones as versatile chiral synthons because of their multi-functionality.[43−46] On the other hand, the mercapto and hydroxyl groups play important roles in biological systems.[47] For instance, the mercapto groups of two cysteine residues can create a cystine unit with a disulfide bond (S−S),[48] which becomes essential to maintain the tertiary and quaternary structure of proteins. Moreover, many biological processes involve oxidation of alcohols to carbonyl compounds[49] (e.g., the ethanol is metabolized to acetaldehyde by the alcohol dehydrogenase enzyme).

Thus, a complete characterization of the reactivity and electronic properties of the alcohol and thiol groups in medium

* To whom correspondence should be addressed. E-mail: mts@iqc.udg.es.

10.1021/jp060664g CCC: $33.50
Published on Web 06/15/2006

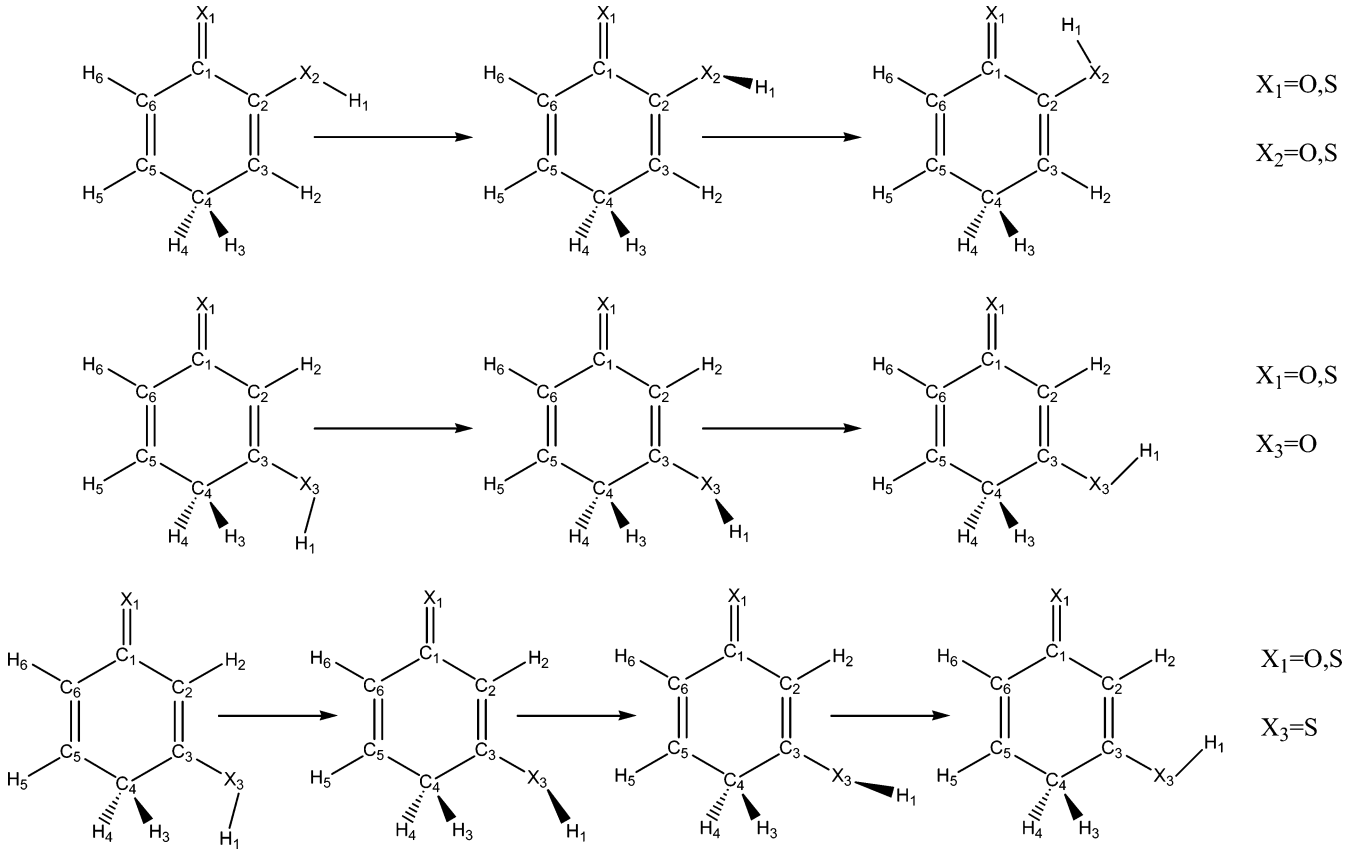

Figure 1. Schematic representation of the pathways corresponding to the internal rotations studied in this work.

size molecules is essential to provide a firm basis for a molecular understanding of the biochemical behavior in larger systems. In particular, the present study is devoted to the analysis of the interconversion between different conformers of the hydroxyl and mercapto derivatives of cyclohexa-2,5-dienone and cyclohexa-2,5-dienthione. The comparative analysis of the rotational behavior of thiol and alcohol groups may provide new insights on the specific reactivity of these chemical groups. It is worth noting that the alcohols (thiols) studied in this paper can be conjugated with the adjacent carbon═carbon double bond with the possible keto−enol (thione−thiol) tautomerism, one of the oldest and most studied topics in physical organic chemistry.[47]

In addition to energetic and electronic characterizations, we are also interested in principles, theorems, or rules that rationalize the chemical reactivity. Among them, one of the most important is the maximum of hardness principle (MHP).[50−54] This principle affirms that systems tend to a state of maximum hardness at constant temperature, external potential, and chemical potential. The MHP has been successfully applied on different types of chemical reactions,[55] although some failures have also been reported.[56,57] Moreover, the hardness profile may play a key role in characterizing the rotational behavior of a given system, for instance, the profiles of reactivity descriptors such as hardness, chemical potential, and electrophilicity might be used to rationalize the energetic data.[58−62] Then, an additional goal of this paper is to evaluate the behavior of the hardness profiles in connection with the torsional energy profiles of molecules where different competing effects (conjugation, hyperconjugation, and steric repulsions) are present and may challenge the validity of MHP on these particular systems.

Computational Details

All quantum chemical calculations were carried out with the aid of the Gaussian 98 set of programs.[63] All geometries were optimized using density functional theory (B3LYP hybrid functional)[64−66] with the 6-311++G(d,p) basis set[67] and characterized at this level by harmonic vibrational frequencies as a minimum or saddle point. Moreover, these calculations were also used to determine the zero-point vibrational energy (ZPVE), absolute entropies, and temperature corrections to calculate enthalpies (H) and free energies (G) at $T = 298$ K. To take into account anharmonic effects, the ZPVEs computed at the B3LYP/6-311++G(d,p) level were scaled by 0.9806.[68] In addition, we performed single point HF, MP2, and MP4 calculations using the 6-311++G(d,p) basis set at the B3LYP/6-311++G(d,p) optimized geometries to study the effect of introducing electron correlation with perturbative methods and to check B3LYP barrier energies.

In a recent article, one of the present authors[69] has shown that the common B3LYP calculations underestimate energy barriers in a series of prototypical reactions, although they yield geometrical parameters for minima and transition states with a quality similar to that provided by the QCISD method. With these results in mind, we have decided to optimize our geometries at the B3LYP/6-311++G(d,p) level and for energies to perform MP4/6-311++G(d,p) single point calculations at the optimized B3LYP/6-311++G(d,p) geometries. With this MP4/6-311++G(d,p)//B3LYP/6-311++G(d,p) method, we expect to obtain results similar to those given by the QCISD and CCSD methodologies.[70]

To quantify the degree of conjugation and hyperconjugation, we used the natural bond orbital (NBO) theory of Reed and Weinhold.[71] The NBO procedure generates first a basis set of orthogonalized and localized one- and two-center cores, lone pairs, and bond orbitals, plus antibonding and Rydberg orbitals that describe the Lewis-like molecular bonding pattern of electron pairs in an optimally compact form. Then, the stability energy, $E^{(2)}$, associated with delocalization between donor

TABLE 1: Calculated Relative Energies (Δ*E*, kcal/mol), Enthalpies (Δ*H*, kcal/mol), Free Energies (Δ*G*, kcal/mol), and Absolute Entropies (Δ*S*, eu) for Each Rearrangement Reaction[a]

	Δ*E*							
species	B3LYP	HF	MP2	MP4	MP4 + ZPVE[b]	Δ*H*[c]	Δ*G*[c]	Δ*S*
O1O2ts	3.10	1.62	2.88	2.73	2.13	1.91	2.23	−1.06
O1O2a	−8.09	−6.58	−7.13	−6.93	−6.62	−6.78	−6.41	−1.24
S1O2ts	2.95	1.29	2.81	2.64	2.08	1.85	2.17	−1.05
S1O2a	−8.82	−6.59	−7.09	−6.82	−6.71	−6.87	−6.50	−1.27
O1S2ts	3.49	1.55	2.66	2.51	2.15	1.85	2.27	−1.38
O1S2a	−2.95	−1.89	−2.36	−2.13	−2.08	−2.15	−2.00	−0.52
S1S2ts	4.12	1.68	2.99	2.75	2.37	2.09	2.46	−1.24
S1S2a	−2.15	−0.58	−1.34	−1.07	−1.23	−1.28	−1.18	−0.31
O1O3ts	4.05	2.69	3.70	3.60	3.07	2.74	3.32	−1.94
O1O3s	−2.78	−3.39	−2.86	−2.76	−2.41	−2.57	−2.21	−1.21
S1O3ts	4.28	2.99	3.78	3.68	3.12	2.79	3.37	−1.94
S1O3s	−2.69	−3.38	−2.66	−2.60	−2.26	−2.42	−2.07	−1.17
O1S3ts1	0.02	0.05	0.30	0.29	0.06	−0.34	0.48	−2.76
O1S3ts2	2.82	1.66	2.44	2.35	1.99	1.59	2.39	−2.69
O1S3s	−0.67	−0.72	−0.44	−0.37	−0.25	−0.35	−0.05	−0.99
S1S3ts1	0.02	0.01	0.16	0.15	−0.13	−0.53	0.29	−2.75
S1S3ts2	3.10	1.82	2.35	2.26	1.85	1.46	2.26	−2.69
S1S3s	−0.69	−0.81	−0.57	−0.53	−0.43	−0.53	−0.23	−1.00

[a] All the relative values are referred to the less stable isomer for each reaction. Geometries and vibrational corrections were calculated at the B3LYP/6-311++G(d,p) level of theory. HF, MP2, and MP4 energies were calculated using the 6-311++G(d,p) basis set with the B3LYP/6-311++G(d,p) optimized geometries. [b] ZPVE is scaled by 0.9806 to take into account the anharmonic effects. [c] MP4 energies with the thermal corrections (298 K) calculated at the B3LYP/6-311++G(d,p) level of theory.

Lewis-type NBOs (i) and acceptor non-Lewis NBOs (j) is approximated by second-order perturbation theory as

$$E^{(2)} = \Delta E_{ij} = q_i \frac{\langle i|\hat{F}|j\rangle}{\epsilon_j - \epsilon_i} \quad (1)$$

where q_i is the donor orbital occupancy, $\hat{F}$ is the Fock operator, and ϵ_j and ϵ_i are NBO orbital energies. $E^{(2)}$ has become an easy and useful tool to quantify and identify conjugation and hyperconjugation interactions. Despite being a powerful technique for studying hybridization and molecular bonding, this methodology has the drawback that the NBO determinantal wave function containing the NBOs with the highest occupation number gives a significantly lower energy than the wave function constructed from the original MOs. As a result, conjugation and hyperconjugation energies are usually overestimated using this approach.[23] However, it is also true that if it is used to compare similar systems or along a reaction coordinate as in the present paper, the results obtained are useful to discuss the trends observed. From a theoretical point of view, using Kohn−Sham (KS) MOs obtained by means of DFT methods in NBO analysis may be questionable because they assume that KS MOs have the same meaning as those obtained at the HF level. However, from a practical point of view, in cases where KS and HF MOs have been compared, KS MOs obtained in DFT approaches are very close to the HF ones.[72−74]

The hardness, η, is a measure of the resistance of a chemical species to change its electronic configuration, and it is defined as the second-order partial derivative of the total electronic energy, E, with respect to the total number of electrons, N.[52,75] Using a finite difference approximation and Koopmans' theorem,[76] one obtains the two most popular working definitions of the hardness

$$\eta_1 = I - A \quad (2)$$

and

$$\eta_2 = \epsilon_{LUMO} - \epsilon_{HOMO} \quad (3)$$

where I and A are the first vertical ionization potential and electron affinity of the neutral molecule, respectively, and ϵ_{LUMO} and ϵ_{HOMO} are the energies of the low unoccupied molecular orbital (LUMO) and the high occupied molecular orbital (HOMO), respectively. In this work, η has been calculated using either eq 2 or eq 3. For the calculation of I and A at the B3LYP/6-311++G(d,p) level, the energy of the cationic and anionic species has been computed using the unrestricted methodology, while the energy of the neutral singlet molecules has been calculated within the restricted formalism.

To follow the variations of the energy, $E^{(2)}$, and η along the chemical processes, we have optimized structures at the B3LYP/6-311++G(d,p) level for each value θ about the ∠C3C2X2H1 (or ∠C2C3X3H1, when the alcohol or thiol group is joined at the C3 atom) dihedral angle. The geometries of these selected points on the path were employed to calculate the energy, $E^{(2)}$, and η of the system.

Results and Discussion

The molecular structures and selected geometrical parameters of the B3LYP/6-311++G(d,p) optimized minima and transition states for all internal rotations analyzed in this work are shown in Figures 2 and 3. Throughout the text, we will use the following notations: 2-hydroxy-cyclohexa-2,5-dienone (O1O2), 2-hydroxy-cyclohexa-2,5-dienethione (S1O2), 2-mercapto-cyclohexa-2,5-dienone (O1S2), 2-mercapto-cyclohexa-2,5-dienthione (S1S2), 3-hydroxy-cyclohexa-2,5-dienone (O1O3), 3-hydroxy-cyclohexa-2,5-dienthione (S1O3), 3-mercapto-cyclohexa-2,5-dienone (O1S3), and 3-mercapto-cyclohexa-2,5-dienthione (S1S3).

Most of the internal rotations studied have two minima at $\theta = 0°$ (syn form) and 180° (anti form) values of the dihedral rotation angle (either ∠C3C2X2H1 for O1O2, S1O2, O1S2, and S1S2 or ∠C2C3X3H1 for O1O3, O1S3, S1O3, and S1S3) and a transition state between these two conformations, except the O1S3 and S1S3 rotations, which show two transition states and two minima. The conformation at $\theta = 180°$ is in these two cases a transition state, and the O1S3 and S1S3 species show very flat minima at $\theta = 167.6$ and 169.8°, respectively.

Energy Analysis. Table 1 summarizes the energetic results obtained for the eight conformational changes studied in this

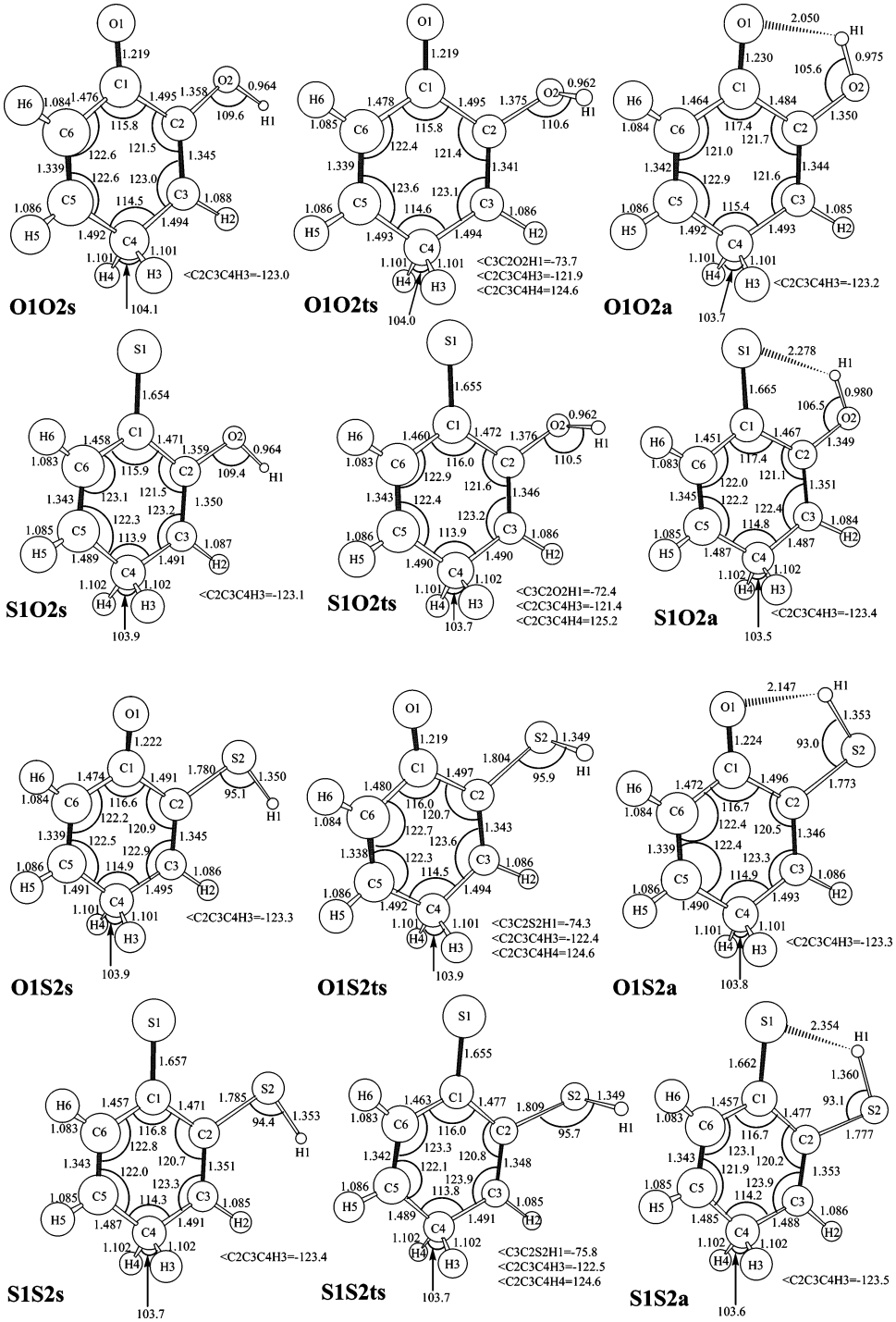

Figure 2. Selected parameters of the B3LYP/6-311++G(d,p) optimized geometries for OH and SH internal rotation around C2. Distances are given in angstroms and angles in degrees.

work. In all of these internal rotations, the reactants and products are defined in such a way that the rearrangement results to be exothermic. The energy differences found between the B3LYP and the MP2 results are smaller than 1 kcal/mol. The average of the difference between the HF and the MP2 energy differences is 0.71 kcal/mol, while for the MP2 and MP4 energy differences, it is 0.13 kcal/mol. Thus, one can conclude that the series of the perturbative methods is almost converged at the MP4 level for energy differences and that the use of more accurate methods will only slightly modify the MP4 energy differences. Throughout the text, all energetic discussion will be referred to energies computed at the MP4 + ZPVE values, where ZPVE has been computed at the B3LYP/6-311++G(d,p) level and has been scaled by 0.9806 to take into account anharmonic effects. In a very recent work, Kahn and Bruice[77] have showed that the MP4(SDQ) level is essential to obtain accurate rotation barriers in small alcohols.

First of all, we will analyze the alcohol and thiol rotation barriers in the X1X2 (X1, X2 = O, S) systems. In these reactions, the anti conformation (X1X2a), anti respect to the C2═C3 bond, is the lower energy structure due to the intramolecular hydrogen bonding between the keto or the thione group with the hydrogen of the hydroxyl or mercapto group. All the relative values quoted in Table 1 are referred to the less stable isomer for each rearrangement reaction; therefore, in the X1X2 systems, the rotational barriers will be related to the energetic

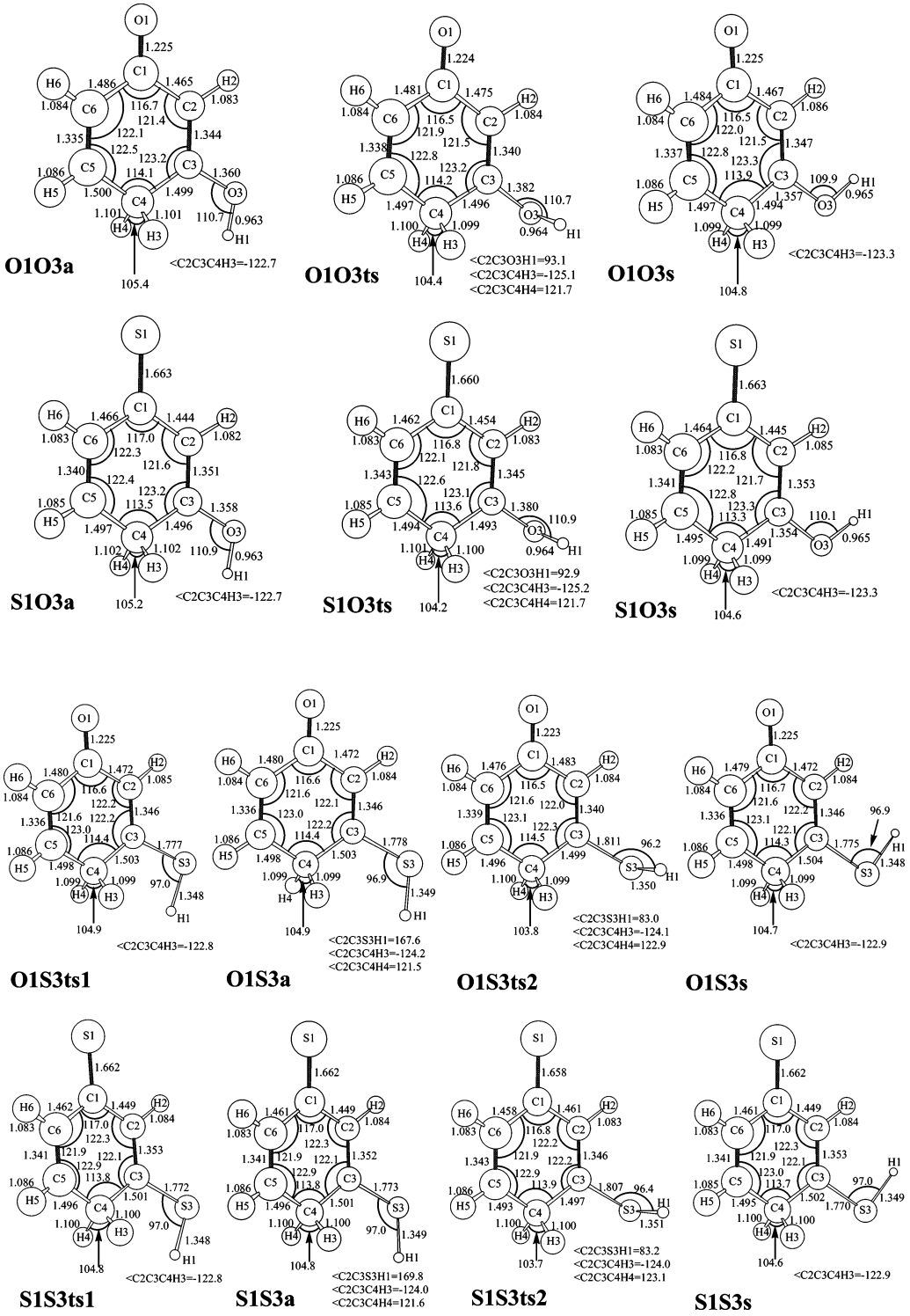

Figure 3. Selected parameters of the B3LYP/6-311++G(d,p) optimized geometries for OH and SH internal rotation around C3. Distances are given in angstroms and angles in degrees.

change between the syn conformations (X1X2s), syn respect to the C2═C3 bond, and the transition state (X1X2ts).

For the X1X2 systems, the energy difference between the syn and the anti conformers is larger for the X1O2 than for the X1S2 species. This is clearly due to stronger hydrogen bonds (H-bonds) produced by the hydroxyl group as compared to those formed by the mercapto group. As a consequence, the energy stabilization for the syn to anti rearrangement is larger for the X1O2 than for the X1S2 species. However, the energetic barrier for the syn to anti conversion is similar for the X1O2 and X1S2 systems (differences less than 0.3 kcal/mol at the MP4 + ZPVE level), and this means that the Pauli repulsions between the electron pairs of the X1 and X2 species are similar for all X1X2 systems.

In contrast to the previous internal rearrangements, the X1X3 systems prefer the syn form (X1X3s) to the anti structure (X1X3a); thus, all relative values related to the X1X3 systems of Table 1 are referred to the anti conformer. Now, one can see that the hydroxyl group shows a somewhat higher (1 kcal/mol) rotational energy barrier than the mercapto group. As before, these energy barriers remain almost unaffected by the modification of the keto group for the thione group, indicating the small

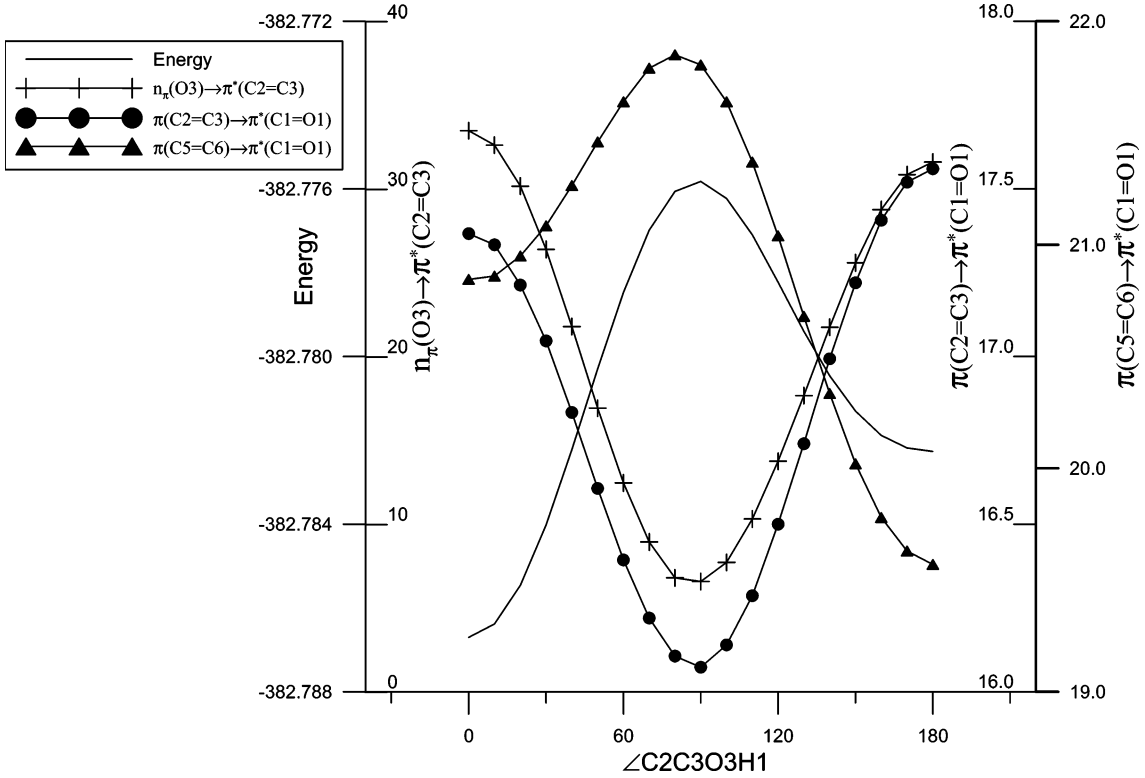

Figure 4. Rotational energy curve (in au) and variations of $E^{(2)}$ for the $n_\pi(O3) \rightarrow \pi^*(C2{=}C3)$, $\pi^*(C2{=}C3) \rightarrow \pi^*(C1{=}O1)$, and $\pi^*(C5{=}C6) \rightarrow \pi^*(C1{=}O1)$ interactions (in kcal/mol) for the 3-hydroxy-cyclohexa-2,5-dienone system along the ∠C2C3O3H1 dihedral angle.

effect of the conjugation of C3═C2 with C1═O1 (or C1═S1) in the rotational energy barrier of the hydroxyl or mercapto group. Because of the lack of H-bonding and repulsion between the lone pairs of X1 and X3, the torsional potential energy is mainly the result of the interactions of the hydroxyl or mercapto group with the C2═C3 double bond.

Natural Bond Orbital Analysis. The effects of conjugation and hyperconjugation along the internal rotations can be evaluated qualitatively in terms of bond lengths or quantitatively using the NBO approach. The origin of the energy difference between the syn and the anti conformer for the X1X2 species is definitely attributed to the H-bond that is formed in the anti form. Less clear is the origin of the higher stabilization of the syn form in the X1X3 species. In this latter case, it is useful to apply the NBO method by removing specific interactions in the anti and syn structures.[1] If the $n_\pi(O3) \rightarrow \pi^*(C2{=}C3)$ is removed in the O1O3a and O1O3s conformers, the energetic difference between the two conformers is reduced from 2.78 to 1.15 kcal/mol (B3LYP/6-311++G(d,p) values). Thus, one can conclude that this hyperconjugation is essential to explain the origin of the energy stabilities. Moreover, the deletion of the anomeric effects $n_\sigma(O3) \rightarrow \sigma^*(C3{-}C4)$ and $n_\sigma(O3) \rightarrow \sigma^*(C2{=}C3)$ of the anti and syn forms produces a further reduction of 0.5 kcal/mol in the energy difference between the two conformers. Finally, if one removes all electron charge transfer from bonds and lone pairs to antibonding NBOs and Rydberg orbitals, the anti form becomes more stable than the syn conformer by 0.26 kcal/mol. Thus, if only the steric interactions (the Pauli repulsions between the lone pairs in the O3 or the O3−H1 bond pair with the C2−H2 or C4−H bond pairs) are taken into account, the anti structure will become the most stable conformer. This result shows that conjugation and hyperconjugation play a key role for understanding the larger stability of the syn form as compared to the anti conformer in the X1X3 species. It is worth nothing that similar conclusions have been obtained for the O1S3, S1O3, and S1S3 systems.

Figure 4 contains a NBO analysis for the O1O3 system along the ∠C2C3O3H1 dihedral angle, while Figures 5 and 6 display some variations of the bond lengths for the same system and dihedral angle. One can see that the conjugation due to the $n_\pi(O3) \rightarrow \pi^*(C2{=}C3)$ interaction in the syn structure is 1.9 kcal/mol stronger than in the anti form, resulting in a net stabilization of the syn conformer. This fact implies that the resonance form R═O3$^+$−H1 and its conjugation with the double bond (C2═C3) will be more important in the syn than in the anti form, explaining the behavior of the C3−O3 and C2═C3 bond distances along the ∠C2C3O3H1 dihedral angle. At the anti structure ($\theta = 180°$), the shape of the $n_\pi(O3)$ and $\pi^*(C2{=}C3)$ NBOs allows a good interaction between them; however, around $\theta = 90°$, their overlap and the $E^{(2)}$ are close to zero. In VB language, this means that the weight of the resonance form R═O3$^+$−H1 has been clearly reduced, and in the MO theory, one can say that the conjugation of the O3 electron pairs and C2═C3 has almost disappeared. From a structural point of view, this is translated into an increase and a reduction of the C3−O3 and C2═C3 bond lengths, respectively. After $\theta = 90°$, the orientation of these orbitals again becomes favorable to interact with each other, generating a stabilization of the system and a reduction and an increase of the C3−O3 and C2═C3 bond lengths, respectively. Finally, the better overlap between these orbitals in the syn structure ($\theta = 0°$) results in shorter C3−O3 (0.003 Å) and longer C2═C3 (0.002 Å) bond lengths than in the anti structure.

On the other hand, the variation of the C5═C6 bond length along the ∠C2C3O3H1 dihedral angle shows the opposite trend observed in the C2═C3 bond distance. The C1−C2 and C1−C6 bond distances present also an opposite behavior. These trends can be rationalized by analyzing the conjugation of

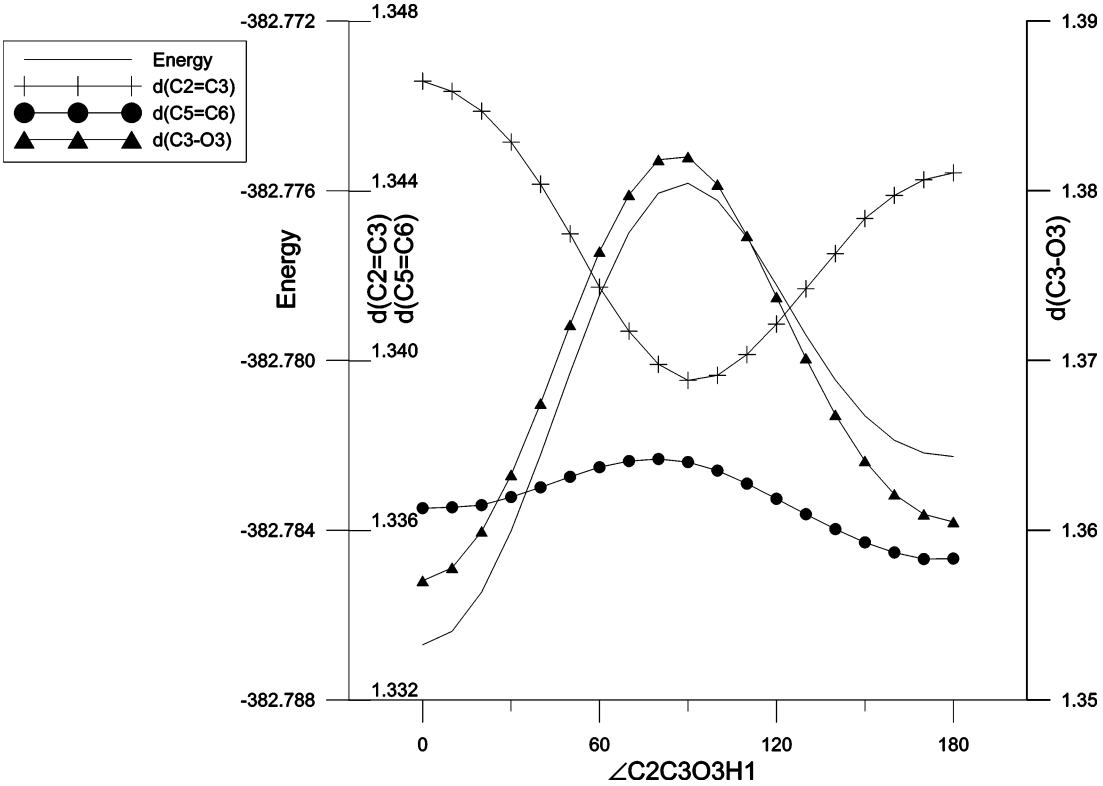

Figure 5. Rotational energy curve and variations of the C2═C3, C5═C6, and C3−O3 bond lengths for the 3-hydroxy-cyclohexa-2,5-dienone system along the ∠C2C3O3H1 dihedral angle. Energy is given in atomic units and distances in angstroms.

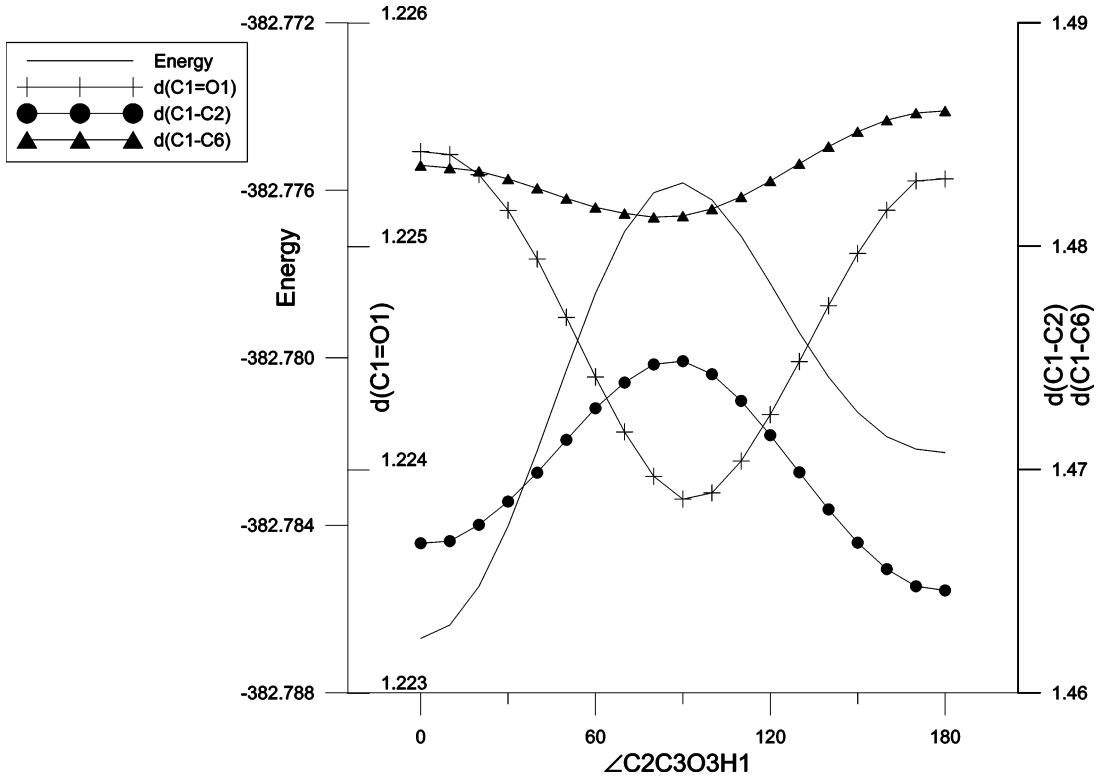

Figure 6. Rotational energy curve and variations of the C1═O1, C1−C2, and C1−C6 bond lengths for the 3-hydroxy-cyclohexa-2,5-dienone system along the ∠C2C3O3H1 dihedral angle. Energy is given in atomic units and distances in angstroms.

C5═C6 and C2═C3 with C1═O1 (i.e., the $E^{(2)}$ variation of $\pi(C2{=}C3) \rightarrow \pi^*(C1{=}O1)$ and $\pi(C5{=}C6) \rightarrow \pi^*(C1{=}O1)$ interactions along the rotation of the hydroxyl group). Figure 4 shows that the interaction between the $\pi(C2{=}C3)$ and the $\pi^*(C1{=}O1)$ NBOs diminishes at the transition state and increases at the syn and anti forms, being stronger at the $\theta =$ 180 than 0°. This is the reason for the presence of the maximum and minimum of the C1−C2 bond length at $\theta = 90$ and 180°, respectively.

In contrast, the $\pi(C5{=}C6) \rightarrow \pi^*(C1{=}O1)$ interaction shows the opposite behavior; thus, it increases around the transition state and diminishes at the minima structures. A smaller

conjugation of C1═O1 with C2═C3 implies that the lone pairs of O1 and the π electrons of C1═O1 become more free to conjugate with C5═C6, producing a lengthening of the C5═C6 and a shortening of the C1−C6 distances at $\theta = 90°$. Moreover, the better conjugation of the $\pi(C2{=}C3) \rightarrow \pi^*$ $(C1{=}O1)$ interaction at the anti structure induces a weaker $\pi(C5{=}C6) \rightarrow \pi^*$ $(C1{=}O1)$ conjugation and C5═C6 and C1−C6 become shorter and longer, respectively, in the anti as compared to the syn form. As far as the C1═O1 bond length is concerned, the $\pi(C5{=}C6) \rightarrow \pi^*$ $(C1{=}O1)$ interaction brings about a shorter bond length at the minima, while the $\pi(C2{=}C3) \rightarrow \pi^*$ $(C1{=}O1)$ causes a lengthening of the C1═O1 bond distance; this last interaction being the most important.

The bond lengths and NBO trends of S1O3 are very similar to O1O3, except that the more delocalized lone electron pairs of the sulfur atom allow a better conjugation of C1═S1 with the C2═C3 and C5═C6 double bonds than C1═O1. Thus, the $\pi(C2{=}C3) \rightarrow \pi^*$ $(C1{=}S1)$ and $\pi(C5{=}C6) \rightarrow \pi^*$ $(C1{=}S1)$ interactions show higher $E^{(2)}$ values than the previous system (O1O3), although the $n_\pi(O3) \rightarrow \pi^*(C2{=}C3)$ interaction and the energetic rotational barrier remain identical.

The behavior of the bond lengths and NBOs along the ∠C2C3S3H1 dihedral angle (O1S3 and S1S3) is analogous to the rotation of the hydroxyl group; however, the long distance of the C3−S3 bond (1.8 Å) leads to less important interactions between the lone pair of the sulfur and the σ and π antibonding NBOs of C2═C3 as compared to the previous cases with the hydroxyl group. This effect is reflected in a reduction of the $E^{(2)}$ values of $n_\pi(S3) \rightarrow \pi^*(C2{=}C3)$ conjugation and the $n_\sigma(S3) \rightarrow \sigma^*(C2{=}C3)$ and $n_\sigma(S3) \rightarrow \sigma^*(C3{=}C4)$ hyperconjugations with the corresponding diminution of the rotational energy barrier. Moreover, these smaller conjugation and hyperconjugation effects result in small geometrical changes along the rotation of the mercapto group. Finally, it is worth noting that the combination of different competing effects (conjugation, hyperconjugation, and steric repulsions) produces the nonplanar structures for the anti conformers (O1S3a and S1S3a).

Hardness and the Maximum Hardness Principle. There is a large bibliography related to the qualitative and quantitative characterization of the energy barrier with different conceptual DFT reactivity indices, especially hardness and chemical potential.[58−62,78−81] For the present systems, we have found that the hardness profiles along the ∠C3C2X2H1 and ∠C2C3X3H1 dihedral angles differ very much for the different species. Thus, while the internal rotation of the XH1 group in the S1O2, S1S2, O1O3, and S1O3 species follows MHP (i.e., energy minima correspond approximately to hardness maxima and vice versa), the same rotation in the O1O2, O1S2, and O1S3 systems breaks it. These results reinforce the conclusion by Chandra and Uchimaru[82] about the fact that the general applicability of MHP along any reaction coordinate is not possible. The constraints required for MHP to be valid (constant external and chemical potentials)[54] are not fulfilled along any reaction coordinate, and therefore, the validity of MHP has to be analyzed in each particular case. In addition, it is worth remarking that the success or failure of MHP must be discussed for the whole reaction coordinate and not by just looking the hardness values at the stationary points of the energy because the hardness maximum or minimum does not necessarily have to coincide with the position of the stationary points of the potential energy surface (PES). For instance, taking into account the values in Table 2 for the energetic stationary points only, one could infer that the rotation in the O1O3 species breaks and follows MHP according to the η_1 and η_2 values, respectively. However, the study of the full η_1 and η_2 profiles along the ∠C2C3O3H1 dihedral angle (see Figure 7) shows that the two hardness profiles fulfill MHP. This characteristic is also present in the hardness values of the O1O2, S1O3, and O1S3 systems. Thus, we can conclude that the exploration of the hardness along the intrinsic reaction coordinate becomes essential to decide if a reaction follows or breaks MHP.

TABLE 2: B3LYP/6-311++G(d,p) Hardness for All Energetic Stationary Points Studied in This Paper[a]

species	η_1	η_2	species	η_1	η_2
O1O2a	0.3331	0.1819	O1O3a	0.3308	0.1851
O1O2ts	0.3330	0.1826	O1O3ts	0.3321	0.1845
O1O2s	0.3250	0.1693	O1O3s	0.3366	0.1876
S1O2a	0.2592	0.1158	S1O3a	0.2615	0.1195
S1O2ts	0.2588	0.1154	S1O3ts	0.2618	0.1191
S1O2s	0.2740	0.1330	S1O3s	0.2638	0.1215
			O1S3ts1	0.3178	0.1761
O1S2a	0.3098	0.1601	O1S3a	0.3166	0.1760
O1S2ts	0.3204	0.1710	O1S3ts2	0.3170	0.1767
O1S2s	0.3030	0.1536	O1S3s	0.3193	0.1778
			S1S3ts1	0.2528	0.1174
S1S2a	0.2586	0.1201	S1S3a	0.2527	0.1173
S1S2ts	0.2489	0.1115	S1S3ts2	0.2541	0.1164
S1S2s	0.2594	0.1244	S1S3s	0.2535	0.1182

[a] η_1 and η_2 are calculated using eqs 2 and 3, respectively. All values are in au.

It is worth noting that some η_1 profiles present irregular trends with problems to mimic the η_2 shapes (e.g., O1O3 of Figure 7). This problem arises from the π conjugated structures of the studied systems and the multi-configuration character of their $N + 1$ and $N - 1$ electronic states. Obviously, this problem could be overcome using a multiconfiguration method like MCSCF, but this is out of the scope of this paper.

In contrast to the previous systems studied, the rotational η_1 and η_2 hardness profiles of the S1S3 molecule display an opposite trend (see Figure 8). While the S1S3s and S1S3ts2 structures are close to the maximum and minimum of η_2, respectively, they become the minimum and maximum for η_1. Moreover, the η_1 profile is the only one that shows the correct number of energetic stationary points along the PES.[83,84] Thus, in this case, one can consider the $I - A$ approximation to be of better-quality than the $\epsilon_{LUMO} - \epsilon_{HOMO}$ one.

The breakdown of MHP according to η_2 for O1O2, O1S2, and O1S3 can be understood by analyzing the trend of the HOMO along the internal rotation (the LUMO shape and energy remain approximately constant). In Figure 9, one can see the HOMO shape for three O1O2 structures, which corresponds to the maximum ($\theta = 120°$ along the ∠C3C2O2H1 dihedral angle) and the two minima ($\theta = 0°$ and $\theta = 180°$) of η_2. At the $\theta = 0°$ and $\theta = 180°$ structures, the HOMO energy is determined in part by the antibonding interaction between the bonding $\pi(C2{=}C3)$ and the lone pair of the O2, while at the 120° structure, one can see that the bonding $\pi(C2{=}C3)$ has been diminished and that the lone pair of the O2 now shows a bonding interaction with the lone pair of the O1. This fact produces a stabilization of the HOMO energy and the correspondent breakdown of the MHP.

Finally, as to the applicability of the minimum polarizability principle (MPP) introduced by Chattaraj and Sengupta[85] on the basis of MHP and the inverse relationship between hardness and polarizability, we have found that there is not a one-to-one mapping of the stationary points in the energy and polarizability profiles along the reaction coordinate. Consequently, the MPP is usually disobeyed, and in general, polarizability profiles have

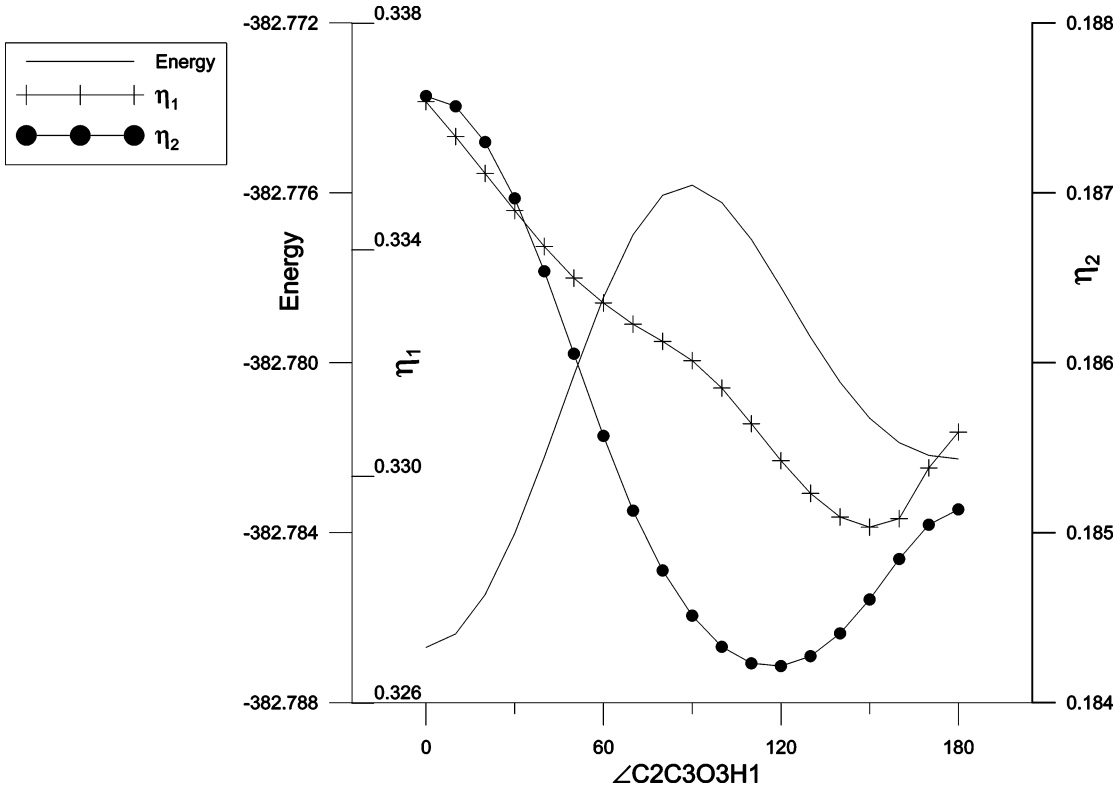

Figure 7. Profiles of energy and hardness for the 3-hydroxy-cyclohexa-2,5-dienone system along the ∠C2C3O3H1 dihedral angle. All values are in atomic units. η_1 and η_2 have been calculated using eqs 2 and 3, respectively.

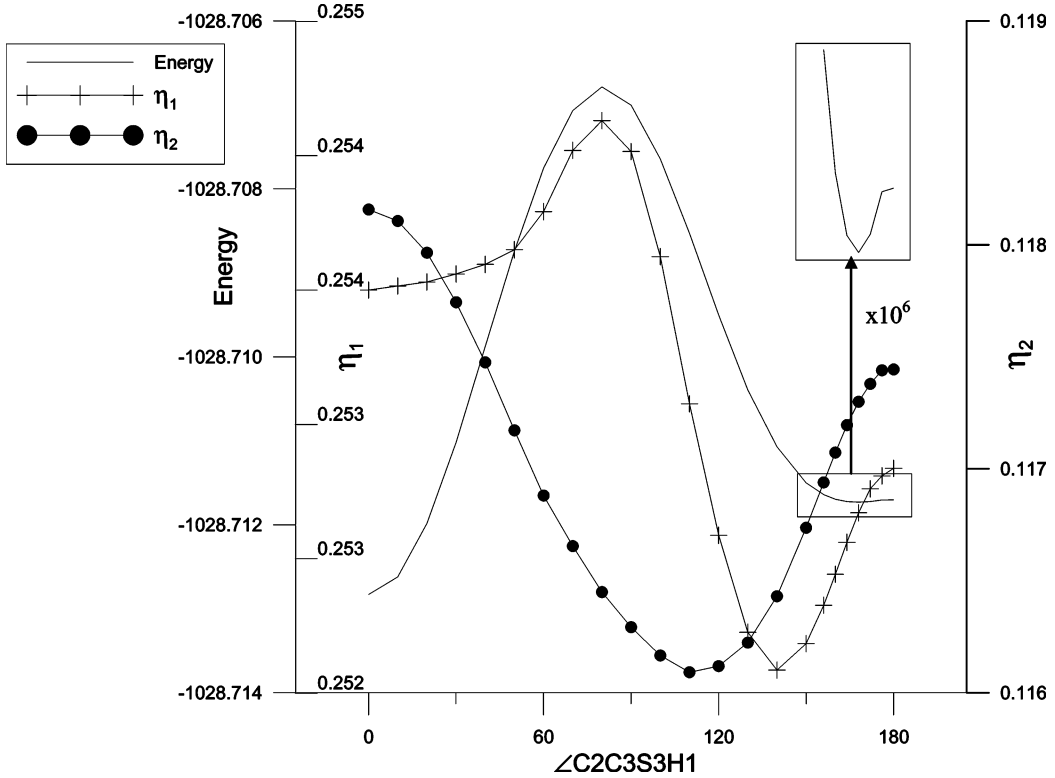

Figure 8. Profiles of energy and hardness for the 3-mercapto-cyclohexa-2,5-dienthione system along the ∠C2C3S3H1 dihedral angle. All values are in atomic units. η_1 and η_2 have been calculated using eqs 2 and 3, respectively.

less interest than their analogous hardness profiles discussed in the present text.

Conclusion

In this paper, the internal rotation of the hydroxyl and mercapto groups has been studied in two different positions (C2 and C3) of cyclohexa-2,5-dione and cyclohexa-2,5-dienthione. The intramolecular H-bonding between the keto or the thione group with the hydrogen of the hydroxyl or mercapto group explains the larger stability of the anti form in the X1X2 species. On the other hand, the interplay between attractive (conjugation and hyperconjugation) and repulsive (steric) interactions around

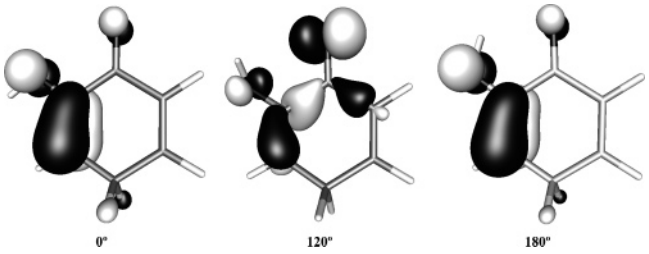

Figure 9. Representation of the B3LYP/6-311++G(d,p) isosurfaces −0.07 (black) and 0.07 (gray) au of the HOMO for 0, 120, and 180° ∠C3C2O2H1 dihedral angles of the 2-hydroxy-cyclohexa-2,5-dienone system.

C3 turns out the syn structure as the lower energy structure. The conjugation and hyperconjugation effects have been evaluated in terms of bond lengths and NBOs. We have shown that the rotational energy barrier is mainly due to $n_\pi(X3) \rightarrow \pi^*(C2{=}C3)$ and the anomeric interactions. Finally, these internal rearrangements have also been characterized by hardness profiles. We have found that some internal rotations follow MHP while others do not. For some particular cases in which MHP is disobeyed, it has been possible to understand the origin of the MHP breakdown.

Acknowledgment. Financial help has been furnished by the Spanish MEC Project CTQ2005-08797-C02-01/BQU and by the Catalan Departament d'Universitats, Recerca i Societat de la Informació (DURSI) through Project 2005SGR-00238. An AIRE grant from the Departament d'Universitats, Recerca i Societat de la Informació (DURSI) of the Generalitat de Catalunya is acknowledged. A.T.L. acknowledges financial support from Projects Fondecyt Nos. 1020534 and 1060590 and from CIMAT (Centro para la Investigación Interdisciplinaria Avanzada en Ciencias de los Materiales), Project FONDAP No. 11980002.

Note Added after ASAP Publication. This Article was published on Articles ASAP on June 15, 2006. A change was made to the fifth sentence of the "Natural Bond Orbital Analysis" section of the Results and Discussion. The corrected Article was posted June 20, 2006.

References and Notes

(1) Weinhold, F.; Landis, C. R. *Valency and Bonding: A Natural Bond Orbital Donor−Acceptor Perspective*; Cambridge University Press: Cambridge, 2005.
(2) Mulliken, R. S. *J. Phys. Chem.* **1933**, *37*, 2.
(3) Bocca, C. C.; Pontes, R. M.; Basso, E. A. *J. Mol. Struct.* **2004**, *710*, 105.
(4) Carneiro, J. W. D.; Dias, J. F.; Tostes, J. G. R.; Seidl, P. R.; Taft, C. A. *Int. J. Quantum Chem.* **2003**, *95*, 322.
(5) Cramer, C. J. *J. Mol. Struct.* **1996**, *370*, 135.
(6) Laube, T. *Angew. Chem., Int. Ed. Engl.* **1986**, *25*, 349.
(7) Foster, J. P.; Weinhold, F. *J. Am. Chem. Soc.* **1980**, *102*, 7211.
(8) Pophristic, V.; Goodman, L. *Nature* **2001**, *411*, 565.
(9) Venkataraman, H.; Cha, J. K. *Tetrahedron Lett.* **1989**, *30*, 3509.
(10) Houk, K. N.; Paddonrow, M. N.; Rondan, N. G.; Wu, Y. D.; Brown, F. K.; Spellmeyer, D. C.; Metz, J. T.; Li, Y.; Loncharich, R. J. *Science* **1986**, *231*, 1108.
(11) Lambert, J. B.; Nienhuis, R. J. *J. Am. Chem. Soc.* **1980**, *102*, 6659.
(12) Craig, N. C.; Kliewer, M. A.; Shih, N. C. *J. Am. Chem. Soc.* **1979**, *101*, 2480.
(13) Houle, F. A.; Beauchamp, J. L. *J. Am. Chem. Soc.* **1979**, *101*, 4067.
(14) Berman, D. W.; Anicich, V.; Beauchamp, J. L. *J. Am. Chem. Soc.* **1979**, *101*, 1239.
(15) Wolfe, S. *Acc. Chem. Res.* **1972**, *5*, 102.
(16) Goodman, L.; Gu, H. B.; Pophristic, V. *J. Phys. Chem. A* **2005**, *109*, 1223.
(17) Juaristi, E.; Cuevas, G. *The Anomeric Effect*; CRC Press: London, 1995.
(18) Amos, D. T.; Renslo, A. R.; Danheiser, R. L. *J. Am. Chem. Soc.* **2003**, *125*, 4970.
(19) Ma, B. Y.; Schaefer, H. F.; Allinger, N. L. *J. Am. Chem. Soc.* **1998**, *120*, 3411.
(20) Shiner, C. S.; Garner, C. M.; Haltiwanger, R. C. *J. Am. Chem. Soc.* **1985**, *107*, 7167.
(21) Erhardt, J. M.; Grover, E. R.; Wuest, J. D. *J. Am. Chem. Soc.* **1980**, *102*, 6365.
(22) Mo, Y. R.; Wu, W.; Song, L. C.; Lin, M. H.; Zhang, Q.; Gao, J. L. *Angew. Chem., Int. Ed.* **2004**, *43*, 1986.
(23) Bickelhaupt, F. M.; Baerends, E. J. *Angew. Chem., Int. Ed.* **2003**, *42*, 4183.
(24) Blom, C. E.; Gunthard, H. H. *Chem. Phys. Lett.* **1981**, *84*, 267.
(25) Leibold, C.; Oberhammer, H. *J. Am. Chem. Soc.* **1998**, *120*, 1533.
(26) Turecek, F.; Cramer, C. J. *J. Am. Chem. Soc.* **1995**, *117*, 12243.
(27) Smith, B. J.; Nguyen, M. T.; Bouma, W. J.; Radom, L. *J. Am. Chem. Soc.* **1991**, *113*, 6452.
(28) Turecek, F.; Brabec, L.; Korvola, J. *J. Am. Chem. Soc.* **1988**, *110*, 7984.
(29) Rodler, M.; Blom, C. E.; Bauder, A. *J. Am. Chem. Soc.* **1984**, *106*, 4029.
(30) Plant, C.; Boggs, J. E.; Macdonald, J. N.; Williams, G. A. *Struct. Chem.* **1992**, *3*, 3.
(31) Umar, Y.; Jimoh, T.; Morsy, M. A. *J. Mol. Struct.* **2005**, *725*, 157.
(32) Zhu, L.; Chen, C. J.; Bozzelli, J. W. *J. Phys. Chem. A* **2000**, *104*, 9197.
(33) Schultz, A. G.; Antoulinakis, E. G. *J. Org. Chem.* **1996**, *61*, 4555.
(34) Evans, D. A.; Cain, P. A.; Wong, R. Y. *J. Am. Chem. Soc.* **1977**, *99*, 7083.
(35) Danishefsky, S. J.; Mantlo, N. B.; Yamashita, D. S.; Schulte, G. *J. Am. Chem. Soc.* **1988**, *110*, 6890.
(36) Evans, D. A.; Hoffman, J. M.; Truesdale, L. K. *J. Am. Chem. Soc.* **1973**, *95*, 5822.
(37) Stern, A. J.; Rohde, J. J.; Swenton, J. S. *J. Org. Chem.* **1989**, *54*, 4413.
(38) Solomon, M.; Jamison, W. C. L.; McCormick, M.; Liotta, D.; Cherry, D. A.; Mills, J. E.; Shah, R. D.; Rodgers, J. D.; Maryanoff, C. A. *J. Am. Chem. Soc.* **1988**, *110*, 3702.
(39) Schultz, A. G.; Harrington, R. E.; Holoboski, M. A. *J. Org. Chem.* **1992**, *57*, 2973.
(40) Schultz, A. G.; Harrington, R. E. *J. Org. Chem.* **1991**, *56*, 6391.
(41) Carreno, M. C.; Gonzalez, M. P.; Fischer, J. *Tetrahedron Lett.* **1995**, *36*, 4893.
(42) Genisson, Y.; Tyler, P. C.; Young, R. N. *J. Am. Chem. Soc.* **1994**, *116*, 759.
(43) Takemoto, Y.; Kuraoka, S.; Hamaue, N.; Aoe, K.; Hiramatsu, H.; Iwata, C. *Tetrahedron* **1996**, *52*, 14177.
(44) Hiroya, K.; Kurihara, Y.; Ogasawara, K. *Angew. Chem., Int. Ed. Engl.* **1995**, *34*, 2287.
(45) Jones, P. G.; Weinmann, H.; Winterfeldt, E. *Angew. Chem., Int. Ed.* **1995**, *34*, 448.
(46) Van de Water, R. W.; Hoarau, C.; Pettus, T. R. R. *Tetrahedron Lett.* **2003**, *44*, 5109.
(47) Carey, F. A. *Organic Chemistry*; McGraw-Hill: New York, 2001.
(48) Altamirano, M. M.; Plumbridge, J. A.; Calcagno, M. L. *Biochemistry* **1992**, *31*, 1153.
(49) Groger, H.; Hummel, W.; Buchholz, S.; Drauz, K.; Van Nguyen, T.; Rollmann, C.; Husken, H.; Abokitse, K. *Org. Lett.* **2003**, *5*, 173.
(50) Pearson, R. G. *J. Chem. Educ.* **1987**, *64*, 561.
(51) Pearson, R. G. Chemical Hardness−A historical Introduction. In *Structure and Bonding*; Sen, K., Ed.; Springer-Verlag: Berlin, 1993; Vol. 80, p 1.
(52) Pearson, R. G. *Chemical Hardness: Applications from Molecules to Solids*; Wiley-VCH: Oxford, 1997.
(53) Pearson, R. G. *J. Chem. Educ.* **1999**, *76*, 267.
(54) Parr, R. G.; Chattaraj, P. K. *J. Am. Chem. Soc.* **1991**, *113*, 1854.
(55) Geerlings, P.; De Proft, F.; Langenaeker, W. *Chem. Rev.* **2003**, *103*, 1793.
(56) Torrent-Sucarrat, M.; Luis, J. M.; Solà, M. *Chem.−Eur. J.* **2005**, *11*, 6024.
(57) Torrent-Sucarrat, M.; Luis, J. M.; Duran, M.; Solà, M. *J. Am. Chem. Soc.* **2001**, *123*, 7951.
(58) Zevallos, J.; Letelier, J. R.; Toro-Labbé, A. *J. Phys. Chem. A* **2004**, *108*, 10186.
(59) Toro-Labbé, A. *J. Phys. Chem. A* **1999**, *103*, 4398.
(60) Cardenas-Jirón, G. I.; Gutierrez-Oliva, S.; Melin, J.; Toro-Labbé, A. *J. Phys. Chem. A* **1997**, *101*, 4621.
(61) Cardenas-Jirón, G. I.; Letelier, J. R.; Toro-Labbé, A. *J. Phys. Chem. A* **1998**, *102*, 7864.
(62) Cadet, J.; Grand, A.; Morell, C.; Letelier, J. R.; Moncada, J. L.; Toro-Labbé, A. *J. Phys. Chem. A* **2003**, *107*, 5334.
(63) Frisch, M. J.; Trucks, G. W.; Schlegel, H. B.; Scuseria, G. E.; Robb, M. A.; Cheeseman, J. R.; Zakrzewski, V. G.; Montgomery, J. A.; Stratmann,

R. E.; Burant, J. C.; Dapprich, S.; Millam, J. M.; Daniels, A. D.; Kudin, K. N.; Strain, M. C.; Farkas, O.; Tomasi, J.; Barone, V.; Cossi, M.; Cammi, R.; Mennucci, B.; Pomelli, C.; Adamo, C.; Clifford, S.; Ochterski, J.; Petersson, G. A.; Ayala, P. Y.; Cui, Q.; Morokuma, K.; Salvador, P.; Dannenberg, J. J.; Malick, D. K.; Rabuck, A. D.; Raghavachari, K.; Foresman, J. B.; Cioslowski, J.; Ortiz, J. V.; Baboul, A. G.; Stefanov, B. B.; Liu, G.; Liashenko, A.; Piskorz, P.; Komaromi, I.; Gomperts, R.; Martin, R. L.; Fox, D. J.; Keith, T.; Al-Laham, M.; Peng, C.; Nanayakkara, A.; Challacombe, M.; Gill, P. M. W.; Johnson, B. G.; Chen, W.; Wong, M. W.; Andres, J. L.; Gonzalez, R.; Head-Gordon, M.; Replogle, E. S.; Pople, J. A. *Gaussian 98*, rev. A11: Pittsburgh, PA, 1998.

(64) Becke, A. D. *J. Chem. Phys.* **1993**, *98*, 5648.

(65) Lee, C.; Yang, W.; Parr, R. G. *Phys. Rev. B* **1988**, *37*, 785.

(66) Stephens, P. J.; Devlin, F. J.; Chabalowski, C. F.; Frisch, M. J. *J. Phys. Chem.* **1994**, *98*, 11623.

(67) Hehre, W. J.; Radom, L.; Schleyer, P. v. R.; Pople, J. A. *Ab Initio Molecular Orbital Theory*; Wiley: New York, 1986.

(68) Scott, A. P.; Radom, L. *J. Phys. Chem.* **1996**, *100*, 16502.

(69) Poater, J.; Solà, M.; Duran, M.; Robles, J. *Phys. Chem. Chem. Phys.* **2002**, *4*, 722.

(70) Bento, A. P.; Solà, M.; Bickelhaupt, F. M. *J. Comput. Chem.* **2005**, *26*, 1497.

(71) Reed, A. E.; Curtiss, L. A.; Weinhold, F. *Chem. Rev.* **1988**, *88*, 899.

(72) Stowasser, R.; Hoffmann, R. *J. Am. Chem. Soc.* **1999**, *121*, 3414.

(73) Politzer, P.; Abu-Awwad, F. *Theor. Chem. Acc.* **1998**, *99*, 83.

(74) Salzner, U.; Lagowski, J. B.; Pickup, P. G.; Poirier, R. A. *J. Comput. Chem.* **1997**, *18*, 1943.

(75) Parr, R. G.; Yang, W. *Density-functional theory of atoms and molecules*; Oxford Univesity Press: New York, 1989.

(76) Koopmans, T. *Physica (Utrecht)* **1934**, *1*, 104.

(77) Kahn, K.; Bruice, T. C. *ChemPhysChem* **2005**, *6*, 487.

(78) Herrera, B.; Toro-Labbé, A. *J. Phys. Chem. A* **2004**, *108*, 1830.

(79) Parthasarathi, R.; Padmanabhan, J.; Subramanian, V.; Maiti, B.; Chattaraj, P. K. *J. Phys. Chem. A* **2003**, *107*, 10346.

(80) Pérez, P.; Toro-Labbé, A. *J. Phys. Chem. A* **2000**, *104*, 1557.

(81) Nguyen, L. T.; Le, T. N.; De Proft, F.; Chandra, A. K.; Langenaeker, W.; Nguyen, M. T.; Geerlings, P. *J. Am. Chem. Soc.* **1999**, *121*, 5992.

(82) Chandra, A. K.; Uchimaru, T. *J. Phys. Chem. A* **2001**, *105*, 3578.

(83) Torrent-Sucarrat, M.; Duran, M.; Luis, J. M.; Solà, M. *J. Chem. Sci.* **2005**, *117*, 549.

(84) Torrent-Sucarrat, M.; Luis, J. M.; Duran, M.; Solà, M. *J. Chem. Phys.* **2004**, *120*, 10914.

(85) Chattaraj, P. K.; Sengupta, S. *J. Phys. Chem.* **1996**, *100*, 16126.